Proceedings of the 17th World Congress
The International Federation of Automatic Control
Seoul, Korea, July 6-11, 2008

A Novel Flow Rate Estimation Method using Extended Kalman Filter and Sensor Dynamics Compensation with Automatic Casting Pouring Process

Yoshiyuki Noda * **Yusuke Matsuo** * **Kazuhiko Terashima** *
Yufan Zheng **

* *Department of Production Systems Engineering, Toyohashi University of Technology, Aichi, Japan (e-mail: noda@ syscon.pse.tut.ac.jp).*
** *Department of Electrical and Electronics Engineering, The University of Melbourne, Melbourne, Australia*

Abstract: We describe here a method for estimating the pouring flow rate for tilting-ladle-type automatic pouring systems used in casting industries. To precisely pour molten metal into the mold, controlling the flow rate of liquid flowing out of the ladle is mandatory. However, it is difficult to directly measure the pouring flow rate by using a conventional flow meter, because the flow meter is damaged by the molten metal. Therefore, in this study, we used a soft sensing technique as part of the pouring flow rate estimation system. For estimation of the flow rate, the weight of liquid in the ladle and the tilting angle of the ladle are measured by a load cell and an encoder, respectively. Then, the flow rate is estimated by using an extended Kalman filter and sensor dynamics of the load cell, since in this study, the flow rate model was built as a nonlinear model. The advantage of the proposed system is that the flow rate can be precisely estimated by the load cell and the encoder. The system is easy to construct, and the load cell is not damaged easily, because it does not come in direct contact with the molten metal. The effectiveness of the proposed flow rate estimation method is demonstrated through experiments.

1. INTRODUCTION

The casting industry often uses a pouring process in which molten metal is poured from a ladle into a mold by tilting the ladle. Since the process involves molten metal, the pouring creates a dangerous environment for workers. Therefore, an automatic pouring system has recently been exploited to improve the working environment, Terashima (1998) and Lindsay (1983).

The pouring process requires that molten metal be quickly and precisely poured into a mold and not spill over the sprue cup, Neumann and Trauzeddel (2002), Terashima and Yano (2001). In the present automatic pouring systems, a teaching-and-playback approach has mainly been applied to satisfy such requirements, Watanabe and Yoshida (1992). In this approach, the tilting-ladle motion generated by the operator is detected using an encoder fitted into the motor, and the process is recorded in the memory of a controller. Then, the automatic pouring system duplicates the memorized tilting-ladle motion. However, this approach involves an immense amount of time and effort. Moreover, the present automatic pouring system cannot achieve a high degree of pouring precision due to changes in the pouring conditions.

To solve the problems with the current automatic pouring system, researchers have proposed advanced control systems for the automatic pouring system. To realize highly accurate flow rate control and determine simply the model parameters, a nonlinear flow rate model that uses hydrodynamics and a flow rate control employing the inverse dynamics have been proposed by Noda and Terashima (2007). Moreover, the falling position model of liquid flowing out of the ladle has been derived by the free-fall condition and using the continuous equation, and a falling control system has been developed using the falling position model, Noda and Terashima (2007). Feedback control systems for the liquid level in the sprue cup have been proposed to reduce the pouring time and avoid the overflow of the liquid from the sprue cup, Fujie (1981). However, such studies have a feedforward construction with respect to the pouring flow rate, because it is difficult to detect the flow rate.

A flow rate feedback control using Fuzzy logic has been applied to the automatic pouring system, Shinohara and Morimoto (1992). In the system, an outflow weight is measured by a load cell installed in the pouring machine. The pouring flow rate is obtained indirectly by differentiating the measured outflow weight. However, the measured outflow weight includes much noise and is subject to the load cell's dynamics, which change as the center of gravity of the ladle changes. Therefore, in the conventional method, the pouring flow rate obtained from the outflow weight cannot be measured precisely. It is important to accurately measure the pouring flow rate by holding the pouring condition, and then construct a pouring flow rate feedback control system, Noda and Terashima (2007).

In general, a liquid's flow rate can be measured directly by a flow meter. However, since molten metal's temperature

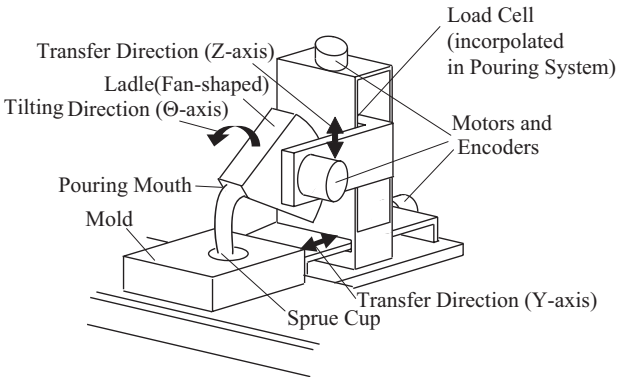

Fig. 1. Tilting-Ladle-Type Automatic Pouring System

is much higher than 1300[deg], the flow meter can be damaged by the molten metal.

Therefore, in this paper, we propose a pouring flow rate estimation method for the casting pouring process that uses a soft sensing technique involving an extended Kalman filter. Most automatic pouring systems in casting plants have a load cell for measuring the outflow weight and an encoder for measuring the tilting angle of the ladle, and the pouring flow rate is estimated by using the outflow weight and the tilting angle of the ladle. The extended Kalman filter algorithm, Corriou (2004) and Reif and Unbehauen (1999) is applied as a nonlinear observer, since the pouring flow rate model is nonlinear. However, another serious problem is that the measured outflow weight by the load cell includes the dynamics incurred by the movement of the gravity center of the ladle. To solve this problem, we estimated the dynamics of the gravity center's movement and subtracted them from the outflow weight.

For experiments, we applied the novel flow rate estimating method to the automatic casting pouring process with a tilting-type ladle. The effectiveness of the proposed method was demonstrated through the experiments.

2. AUTOMATIC POURING SYSTEM

The automatic pouring system with a tilting-type ladle used in this study is shown in Fig. 1. The automatic pouring system can transfer the ladle in two dimensions (Y- and Z-axes) and rotate the ladle (Θ-axis). On the Θ-axis, the ladle is tilted by an AC servomotor. The drive torque of the AC servomotor can be amplified by reducing the gear ratio. The center of the ladle's rotation shaft is placed near the ladle's center of gravity. When the ladle is rotated around the center of gravity, the tip of the pouring mouth moves in a circular trajectory. It is then difficult to pour the molten metal into the mold, as the pouring mouth is moved by tilting. Therefore, the position of the tip of the pouring mouth is controlled invariably during pouring by means of synchronous control of the Y- and Z-axes for rotational motion around the ladle's Θ-axis, Noda and Terashima (2007). The rotation angle is measured by an encoder installed in the AC servomotor. The ladle is also transferred along the Y- and Z-axes of the automatic pouring system by AC servomotors. The driving force of each motor is amplified through a ball and screw mechanism. The ladle can be independently transferred along each axis. In this study, the ladle is fan-shaped. It is easy to control the pouring flow rate using a fan-shaped

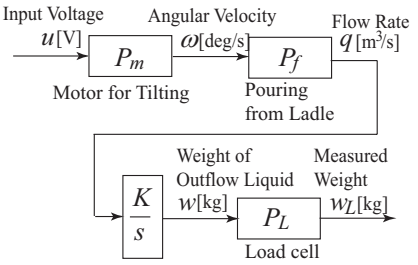

Fig. 2. Block Diagram of Pouring System

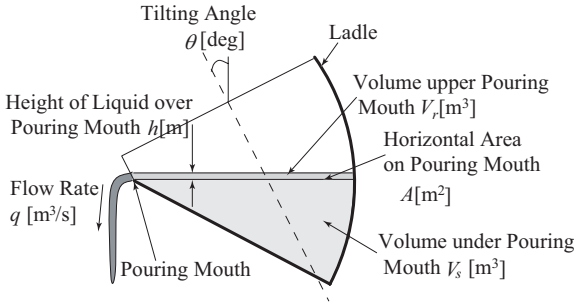

Fig. 3. Cross Section of Pouring Process

ladle because the liquid surface in the ladle is constant at any tilting angle.

To measure the weight of the liquid in the ladle, a load cell is fitted to the arm supporting the ladle in the pouring system. The weight of the liquid in the ladle is obtained by subtracting the weight of the ladle, the motor, and the arm from the total weight measured by the load cell.

3. MODEL OF AUTOMATIC POURING SYSTEM

In the automatic pouring system, an input voltage is applied to the motor for tilting the ladle, and liquid in the ladle is poured into the mold by tilting the ladle. The weight of the outflow liquid is measured by the load cell. The pouring process is represented by the block diagram shown in Fig. 2.

3.1 Motor Model: P_m

In Fig. 2, the motor P_m for tilting the ladle is described as the following first-order system:

$$\frac{d\omega(t)}{dt} = -\frac{1}{T_m}\omega(t) + \frac{K_m}{T_m}u(t), \tag{1}$$

where $\omega(t)$[deg/s] is the angular velocity of the tilting ladle, and u[V] is the input voltage applied to the motor. T_m[s] is the time constant, and K_m[deg/s/V] is the gain.

3.2 Flow Rate Model: P_f

P_f in Fig. 2 is a flow rate model representing the process from the angular tilting velocity to the flow rate of the outflow liquid. This model has been introduced by Noda and Terashima (2007).

A cross section of the pouring process is shown in Fig. 3. In Fig. 3, θ[deg] is the tilting angle of the ladle, $V_s(\theta)$[m^3] is the volume under the pouring mouth, and A[m^2] is the horizontal area to the pouring mouth. The volume $V_s(\theta)$[m^3] changes depending on the tilting angle θ[deg]. V_r[m^3] is the volume over the area A[m^2], and h[m] is the

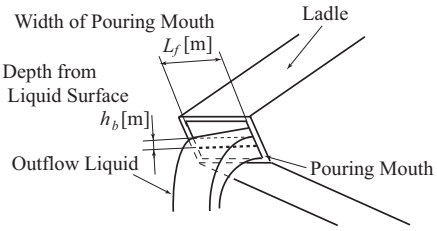

Fig. 4. Detail of Outflow Liquid around Pouring Mouth

height from the area $A[\mathrm{m}^2]$ to the surface of the liquid in the ladle. When the liquid is above the lip of the pouring mouth, the liquid is poured from the ladle, and $q[\mathrm{m}^3/\mathrm{s}]$ is the flow rate of the outflow liquid.

In Fig. 3, the mass balance of the liquid in the ladle is described as follows:

$$\frac{dV_r(t)}{dt} = -q(t) - \frac{dV_s(\theta(t))}{dt}, \tag{2}$$

where $\omega(t)$ is the angular velocity of the tilting ladle. In the fan-shaped ladle, the volume $V_s(\theta)$ is represented as a linear function in relation to the tilting angle. Therefore, Eq. (3) can be expressed as follows:

$$\begin{aligned}\frac{dV_r(t)}{dt} &= -q(t) - \frac{\partial V_s(\theta)}{\partial \theta}\frac{d\theta(t)}{dt} \\ &= -q(t) - DV_s\omega(t), \\ (DV_s &= \frac{\partial V_s(\theta)}{\partial \theta} = \text{constant})\end{aligned} \tag{3}$$

The volume $V_r[\mathrm{m}^3]$ can be represented as follows:

$$V_r(t) \approx Ah(t). \tag{4}$$

Therefore, the height $h[\mathrm{m}]$ is represented as follows:

$$h(t) \approx \frac{V_r(t)}{A}. \tag{5}$$

Using Bernoulli's theorem, the flow rate $q[\mathrm{m}^3/\mathrm{s}]$ at the height $h[\mathrm{m}]$ is shown as follows:

$$q(t) = c\int_0^{h(t)} (L_f\sqrt{2gh_b})dh_b = \frac{2\sqrt{2g}cL_f}{3}h(t)^{3/2}, \quad (0 < c < 1), \tag{6}$$

where $h_b[\mathrm{m}]$ is the depth from the surface of the liquid in the ladle, and $L_f[\mathrm{m}]$ is the width of the pouring mouth, as shown in Fig. 4. In addition, c is the flow rate coefficient, and $g[\mathrm{m}/\mathrm{s}^2]$ is the acceleration of gravity.

From Eqs.(3), (5), and (6), the flow rate model in the pouring process can be derived as follows:

$$\frac{dV_r(t)}{dt} = -\frac{2\sqrt{2g}cL_f}{3A^{3/2}}V_r(t)^{3/2} - DV_s\omega(t), \tag{7}$$

$$q(t) = -\frac{2\sqrt{2g}cL_f}{3A^{3/2}}V_r(t)^{3/2}, \quad (0 < c < 1). \tag{8}$$

In Eqs.(7) and (8), the parameters $DV_s[\mathrm{m}^3/\mathrm{deg}]$, $A[\mathrm{m}^2]$, and $L_f[\mathrm{m}]$ are obtained from the shape of the ladle. Therefore, only the flow rate coefficient c is an unknown parameter and can be identified by performing the experiment only once.

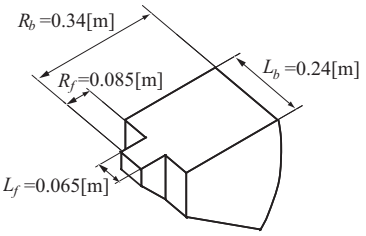

Fig. 5. Configuration of Fan-Type Ladle

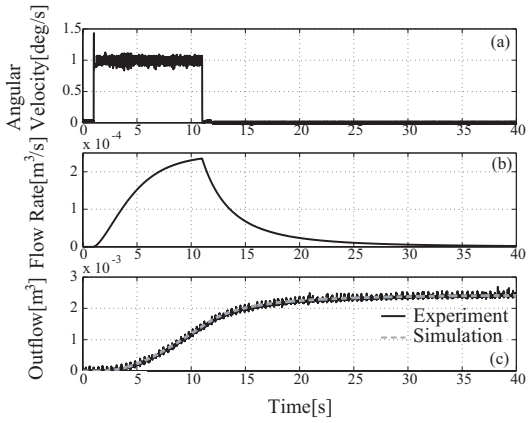

Fig. 6. Experimental Results for Identification of Flow Rate Model

3.3 Load Cell Model:P_L

To express the actual weight $w[\mathrm{kg}]$ of the liquid flowing out of the ladle, the flow rate $q(t)[\mathrm{m}^3/\mathrm{s}]$ is integrated and then multiplied by the liquid's density $\rho[\mathrm{kg}/\mathrm{m}^3]$, as shown in Eq. (9):

$$w(t) = \rho\int_0^t q(\tau)d\tau, \tag{9}$$

The load cell dynamics is represented as a first-order system. Therefore, the load cell model P_L is described as follows:

$$\frac{dw_L}{dt} = -\frac{1}{T_L}w_L(t) + \frac{1}{T_L}w(t), \tag{10}$$

where $w_L(t)[\mathrm{kg}]$ is the weight of the outflow liquid measured by the load cell, and $T_L[\mathrm{s}]$ is the time constant representing the response of the load cell.

3.4 Parameters Identification and Model Verification

We identify the parameters of the motor and the load cell used in the experiments by fitting the results of simulation using the models to the experimental result. The time constant T_m in the motor is $0.6\times10^{-2}[\mathrm{s}]$, and the gain K_m is 24.58[deg/s/V]. The time constant T_L in the load cell is 0.10[s].

The ladle used in this study has the shape shown in Fig. 5. We used water as the target liquid because of safety requirements. Water's density is $\rho = 1.0\times10^3[\mathrm{kg}/\mathrm{m}^3]$. In this experimental condition, the step input u=0.04[V] was applied to the motor for 10[s]. The initial tilting angle of the ladle was 26[deg]. The experimental results are shown in Fig. 6. In Fig. 6, the angular velocity $\omega(t)[\mathrm{deg}/\mathrm{s}]$ is shown in (a), the flow rate $q[\mathrm{m}^3/\mathrm{s}]$ of the outflow liquid in the simulation is shown in (b), and the weights of the

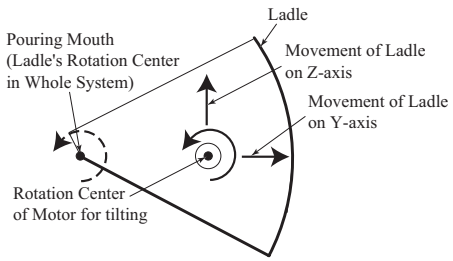

Fig. 7. Virtual Rotation Center to Tilting Ladle System

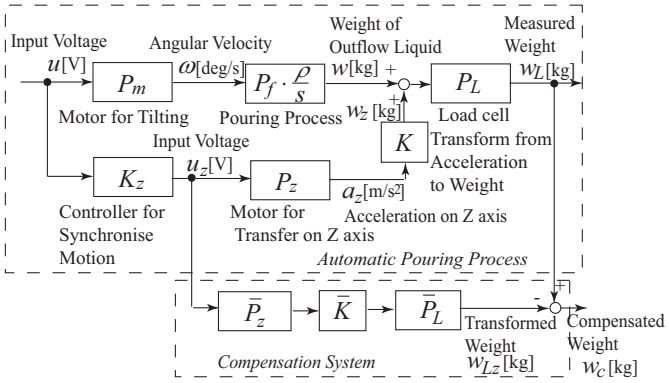

Fig. 8. Compensation System for Measuring Outflow Weight

outflow liquid are shown in (c). The solid line indicates the experimental result, and the dotted line shows the simulation result. By fitting the simulation result to the experimental result in Fig. 6(c), we obtained the flow rate coefficient as c=0.85. The weight of the outflow liquid in the simulation tracks precisely the experimental result, as shown in Fig. 6(c). Moreover, when the other tilting patterns of the ladle were applied to the automatic pouring system, the simulation results generated by the flow rate model tracked precisely to the experimental results, Noda and Terashima (2007). Therefore, the flow rate model represents the actual flow rate in the pouring process, thus validating the model.

4. COMPENSATION OF THE OUTFLOW LIQUID'S WEIGHT MEASURED BY LOAD CELL

In the automatic pouring system shown in Fig.1, the rotation center of the motor for tilting the ladle has been located near the gravity center of the ladle. When the ladle is rotated around the ladle's gravity center, the tip of the pouring mouth is moved in a circular trajectory. In this case, the molten metal is not poured precisely into the mold because of movement of the pouring mouth. Therefore, the ladle is rotated around the tip of the pouring mouth by moving the ladle synchronously along the Y- and Z-axes, as shown in Fig.7.

In this system, the weight data measured by the load cell included the movement of the ladle along the Z-axis, because the load cell is fitted to the arm supporting the ladle, as shown in Fig. 1. To measure only the weight of the outflow liquid, we employed the compensation system shown in Fig. 8. In Fig. 8, the motor P_z on the Z-axis is driven through the controller K_z for synchronous motion. Then, the movement along the Z-axis is added to the load cell data with the weight of the outflow liquid. In the compensation system, the transformed weight w_{Lz}[kg]

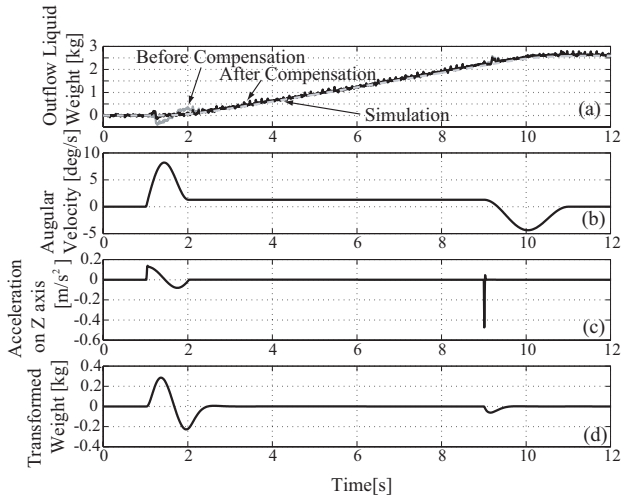

Fig. 9. Experimental Results by using Compensation System

to the movement along the Z-axis is estimated, and then the weight subtracted from the measured weight w_L[kg] as follows:

$$w_c(t) = w_L(t) - w_{Lz}(t). \tag{11}$$

The movement along the Z-axis can be estimated by identifying the motor model P_z as follows:

$$a_z(t) = \frac{dv_z(t)}{dt} = -\frac{1}{T_{mz}} v_z(t) + \frac{K_{mz}}{T_{mz}} u_z(t), \tag{12}$$

where parameters T_{mz} and K_{mz} are identified by fitting the simulation results with the experimental result. We obtained the parameters as T_{mz}=0.007[s] and K_{mz}=0.0828[m/sV].

The load cell model P_L is already represented by Eq. (10). The transformation K from the acceleration a_z[m/s^2] to the weight w_z[kg] is determined as follows:

$$K = M/g, \tag{13}$$

where M[kg] is the total mass of the ladle, the motor, and the supporting arm, and g[m/s^2] is a gravity acceleration. The mass M[kg] is identified by a step response method as M=2.45[kg].

Experimental results by the compensation system are shown in Fig. 9. In Fig. 9, the weights of the outflow liquid are shown in (a), the tilting angular velocity ω[deg/s] of the ladle is shown in (b), the acceleration a_z[m/s^2] of the ladle along the Z-axis is shown in (c), and the transformed weight w_{Lz}[kg] is shown in (d). In Fig. 9(a), the grey solid line represents the weight of the outflow liquid measured by the load cell, the grey dotted line is the outflow liquid weight in simulation using the pouring flow rate model, and the black solid line is the outflow liquid weight after the compensation. The outflow liquid weight measured by the load cell is influenced by the acceleration of the ladle movement along the Z-axis. On the other hand, the outflow liquid weight in simulation is not influenced by the acceleration because there was no consideration of the effect of acceleration along the Z axis. And, in the outflow liquid weight after the compensation, the influence of the acceleration along the Z-axis is almost canceled by the compensation system.

5. AN ESTIMATION METHOD OF CASTING POURING FLOW RATE USING AN EXTENDED KALMAN FILTER

5.1 Extended Kalman Filter

We used a discrete-time extended Kalman filter, Corriou (2004), and Reif and Unbehauen (1999), to estimate to the pouring flow rate. The target system can be represented as follows:

$$z_{n+1} = f(z_n, x_n), \tag{14}$$

$$y_n = h(z_n), \tag{15}$$

where $n \in N_0$ represents the sampling number, and $z_n \in R^q$, $x_n \in R^p$, and $y_n \in R^m$ represent the state, input, and output, respectively. We assumed that the functions f and h were in C^1 function. To Eq. (14) and (15), the extended Kalman filter was formulated as follows:

$$\hat{z}^-_{n+1} = f(\hat{z}^+_n, x_n), \tag{16}$$

$$\hat{z}^+_{n+1} = \hat{z}^-_n + K_n(y_n - h(\hat{z}^-_n)), \tag{17}$$

where the Kalman gain K_n is the $q \times m$ matrix in time varying, and the estimated states $\hat{z}^+_n$ and $\hat{z}^-_n$ are the priori estimate and the posteriori estimate, respectively.

The Kalman gain K_n is updated by the following sequence:

- Time Update:

$$\hat{z}^-_{n+1} = f(\hat{z}^+_n, x_n), \tag{18}$$

$$P^-_{n+1} = A_n P^+_n A^T_n + Q, \tag{19}$$

- Linearization:

$$A_n = \frac{\partial f}{\partial z}(\hat{z}^+_n, x_n), \tag{20}$$

- Measurement Update:

$$\hat{z}^+_n = \hat{z}^-_n + K_n(y_n - h(\hat{z}^-_n)), \tag{21}$$

$$P^+_n = (I - K_n C_n)P^-_n, \tag{22}$$

- Kalman Gain:

$$K_n = P^-_n C^T_n (C_n P^-_n C^T_n + R)^{-1}, \tag{23}$$

- Linearrization:

$$C_n = \frac{\partial h}{\partial z}(\hat{z}^-_n), \tag{24}$$

where Q is the $q \times q$ positive definite symmetric matrix, and R is the $m \times m$ positive definite symmetric matrix. Q and R represent covariance matrices of the system noise and the measurement noise, respectively. In the next section, to estimate the pouring flow rate q[m^3/s], we applied the discrete-time extended Kalman filter to the automatic pouring system.

5.2 Application of an Extended Kalman Filter to the Automatic Casting Pouring System

The models of the automatic pouring process shown in Eqs. (7)-(10) are transformed into the difference equation as follows:

$$z_{n+1} = f(z_n, x_n), \tag{25}$$

$$y_n = h(x_n), \tag{26}$$

$$z_n = [\, V_r(n)\ w(n)\ w_L(n)\,]^T, \quad x_n = \omega(n),$$

$$f(z_n, x_n) = \begin{bmatrix} A_f V_r(n)^{3/2} + V_r(n) + B_f \omega(n) \\ \rho C_f V_r(n)^{3/2} + w(n) \\ e^{-t_s/T_L} w_L(n) + (1 - e^{t_s/T_L}) w(n) \end{bmatrix},$$

$$h(z_n) = w_L(n),$$

$$A_f = C_f = -\frac{2\sqrt{2g}cL_f t_s}{3A^{3/2}}, \quad B_f = -DV_s t_s,$$

where t_s[s] is the sampling interval, and n is the sampling number as $t = nt_s$.

For construction of the extended Kalman filter, the covariance matrices of both Q and R are required. It is assumed that the noise on the weight measured by the load cell has a normal distribution. We then obtain the covariance matrix R of the measuring noise by determining the variance of noise on the weight measured by the load cell. Through the experiments, the variance of the noise is obtained as $R = 1.82 \times 10^{-3}$[kg^2].

The system noise v is represented as follows:

$$v = [\, v_q\ v_w\ v_{wL}\,]^T, \tag{27}$$

where it is assumed that the system noise v has a normal distribution. The variances of system noise are obtained by comparing the outflow liquid weight w_L[kg] in the experiment with that in the simulation by the following equation:

$$z_{n+1} = f(z_n, x_n) + v \tag{28}$$

In this study, with regard to the system noise, we supposed that the starting angle of the outflow from the ladle was different between the design condition and the actual one. We assumed that the maximum error of the starting angle was 3[deg]. In a real casting plant, the maximum error of the starting angle would be less than 3[deg]. Comparing the simulations and the experiment, we obtain the variances of the system noise as Σ_{vq}=1.0×10^{-10}[m^6/s^2], Σ_{vw}=1.0×10^{-6}[kg^2], and Σ_{vwL}=1.0×10^{-6}[kg^2]. Therefore, the covariance Q of the system noise is shown as follows:

$$Q = \begin{bmatrix} \Sigma_{vq} & 0 & 0 \\ 0 & \Sigma_{vw} & 0 \\ 0 & 0 & \Sigma_{vwL} \end{bmatrix}. \tag{29}$$

By using the discrete time model of Eqs. (25) and (26), and the covariances Q and R, we can estimate the flow rate.

5.3 Simulation of Flow Rate Estimation using the Extended Kalman Filter

The simulation results of the flow rate estimation using the extended Kalman filter are shown in Fig. 10. In Fig. 10, the tilting angular velocity ω[deg/s] is shown in (a), the tilting angle θ[deg] is shown in (b), the outflow liquid weight w_L[kg] is shown in (c), and the pouring flow rate is shown in (d). In Fig. 10(c) and (d), the grey lines show the simulation results by using the pouring model of Eqs. (25) and (26), and the black solid lines show the estimation results by using the extended Kalman filter. We found that the estimation results by using the extended Kalman filter accurately track the simulation results of the pouring model.

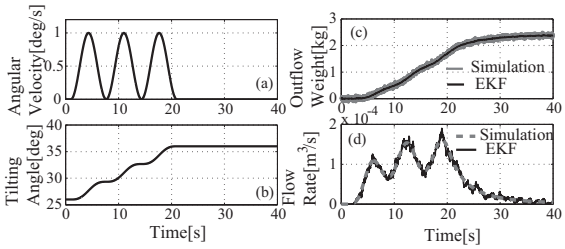

Fig. 10. Simulation Results of Flow Rate Estimation using Extended Kalman Filter

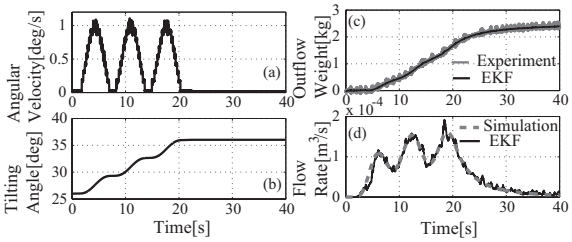

Fig. 11. Experimental Results of Flow Rate Estimation using Extended Kalman Filter

6. EXPERIMENTAL RESULTS

The flow rate estimation system was applied to the automatic pouring system as shown in Fig. 1. The first experiment was performed under the same conditions as were used for the simulation described in the previous section. The experimental results are shown in Fig. 11. Fig. 11(a), (b), (c), and (d) are assigned as Fig. 10. In Fig. 11(c), the grey line is the actual outflow liquid weight in the experiment, and the black line is the estimated outflow liquid weight by the extended Kalman filter. In Fig. 11(d), the grey dotted line is the simulated pouring flow rate by the pouring model, and the black solid line is the estimated pouring flow rate. In the experiment, the pouring flow rate can be estimated by the proposed estimation system.

The next experiments were performed under the conditions in which there were errors between the designed starting angle of the outflow and the real one. The experimental results are shown in Fig. 12. In the experiment, the ladle was tilted with the angular velocity 1.0[deg/s]. In Fig. 12, the angular velocity ω[deg/s] to tilt the ladle is shown in (a) and the tilting angle is shown in (b). The pouring flow rates on errors 0[deg], +1[deg], +3[deg], and +5[deg] of the starting angles to the outflow are shown in Fig. 12(c), (d), (e), and (f), respectively. In the experiments, the time to estimate precisely the pouring flow rate was increased, as was the error of the starting angle to outflow. However, in a few seconds, the pouring flow rate was estimated precisely by the proposed estimation system.

7. CONCLUSIONS

We proposed a pouring flow rate estimation system using an extended Kalman filter and an outflow weight compensation system. In the compensation system, the effect of movement of the ladle along the Z-axis, which is included in the outflow weight, can be canceled by estimating the movement. Then, to estimate the pouring flow rate, we used the design procedure incorporating the extended Kalman filter. Through experiments, we demonstrated that the proposed estimation method is effective in practical use.

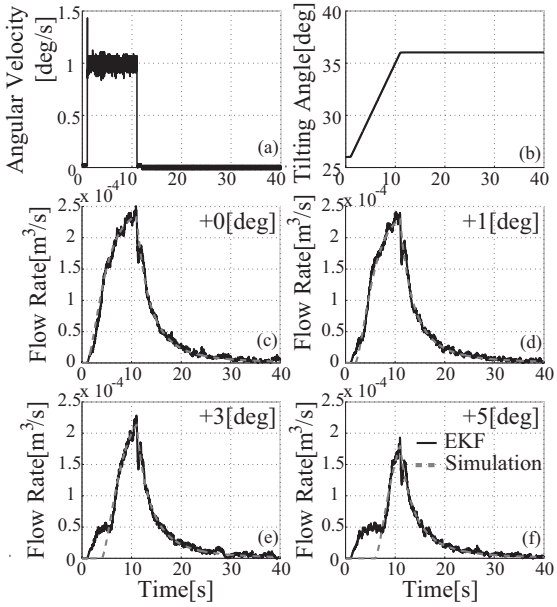

Fig. 12. Experimental Results with Errors of Starting Angle to Outflow

REFERENCES

K. Terashima. Recent automatic pouring and transfer systems in foundries. *Materials Process Technology (in Japanese)*, volume 39, no. 6, pages 1–8, 1998.

W. Lindsay. Automatic pouring and metal distribution systems. *Foundry Trade Journal*, February, no. 6, pages 151–176, 1983.

E. Neumann and D. Trauzeddel. Pouring systems for ferrous applications. *Foundry Trade Journal*, July, pages 23–24, 2002.

K. Terashima and K. Yano. Sloshing Analysis and Suppression Control of Tilting-Type Automatic Pouring Machine. *IFAC Journal of Control Engineering Practice*, volume 9, no. 6, pages 607–620, 2001.

J. Watanabe and K. Yoshida. Automatic pouring equipment for casting "mel pore system". *Industrial Heating (in Japanese)*, volume 29, no. 4, pages 19–27, 1992.

Y. Noda and K. Terashima. Modeling and feedforward flow rate control of automatic pouring system with real ladle. *Journal of Robotics and Mechatronics*, volume 19, no. 2, pages 205–211, 2007.

Y. Noda and K. Terashima. Falling positon control of outflow liquid for automatic pouring system with tilting-type ladle. *Preprints of 12th IFAC Symposium on Automation in Mining, Mineral and Metal Processing*, pages 53–58, 2007.

M. Fujie. Application of microcomputer to automatic pouring. *Journal of the Japan Gereral Foundry Center*, volume 22, no. 10, pages 7–11, 1981.

K. Shinohara and H. Morimoto. Development of automatic pouring equipment. *Journal of the Society of Automotive Engineers of Japan*, volume 46, no. 11, pages 79–85, 1992.

J. Corriou. *Process Control: Theory and Applications*. Springer, London, 2004.

K. Reif and R. Unbehauen. The Extended Kalman Filter as an exponential observer for nonlinear systems. *IEEE Transactions on Signal Processing*, volume 47, no. 8, pages 2324–2328, 1999.